ISSN 8755-6839

SCIENCE OF TSUNAMI HAZARDS

Journal of Tsunami Society International

Volume 36 Number 2 2017

# INVESTIGATION OF b-VALUE VARIATIONS IN THE AFRICAN AND PARTS OF EURASIAN PLATES

**[1]Awoyemi, M. O., [2]Hammed O.S., [1]Shode, O. H., [4]Olurin, O.T., [2]Igboama, W.N. and [3]Fatoba, J.O.**

1. Department of Physics, Obafemi Awolowo University, Ile-Ife, Nigeria.
2. Department of Physics, Federal University, Oye Ekiti, Nigeria.
3. Department of Geophysics, Federal University, Oye Ekiti, Nigeria.
4. Department of Physics, Federal University of Agriculture, Abeokuta, Nigeria.

## ABSTRACT

Numerous earthquakes have occurred along the collision zones of the African and parts of Eurasian plates. Some of these earthquakes along these zones have generated tsunamis. To mitigate this hazard, knowledge of *b*-values of the Gutenberg – Richter relation for tectonic earthquakes in the African and parts of Eurasian plates is essential. The temporal variations of *b*-values were evaluated using sliding time windows with each window containing a total of 100 events with a view to utilizing the results as a precursor for the earthquake occurrence. The spatial variation of *b*-values of the study area was also delineated by dividing it into grids and calculating the *b*-values for each grid using constant radius and constant number of events. Results obtained from the temporal variation of *b*-values showed that earthquakes of large magnitudes occurred when the *b*-values were low while earthquakes of small magnitudes occurred when the *b*-values were high throughout the study period. The results of the spatial distribution of *b*-values also showed that earthquakes of large magnitudes occurred in areas of low *b*-values while earthquakes of small magnitudes occurred in areas of high *b*-values. The study therefore concluded that the temporal and spatial variations of *b*-values might be considered as a precursor for earthquake prediction.

**Keywords**: *b*-value, tsunami, Precursor, Plates, Earthquake, Tectonics.

## 1.0 INTRODUCTION

The occurrence of destructive earthquakes along the collision zone of African and Eurasian plate boundaries had generated tsunamis in past decades. Despite that there are many uncertainties about the relative motions between the tectonic plates of Africa and Eurasia, continuous continental collision, subduction and crustal shortening processes are still occurring in the zone (Pararas-Carayannis, 2011). From the seismo-tectonic history and estimated rates of these tectonic plate collisions, it is very likely that another destructive earthquake and tsunami similar to the 365 AD and 1303 AD events is statistically long overdue and very likely to occur again in the zone. Such great tsunamigenic earthquakes can be expected to occur every 800 years or so along African and Eurasian plate boundaries (Pararas-Carayannis, 2011).

The African plate is one of the major tectonic plates of the earth where few large earthquakes have been reported. At present, the African plate is the fourth largest tectonic plate (~61 H of Eurasia ) a landmass consisting of the traditional continents of Europe and Asia). It also includes oceanic crust extending westward to the Mid - Atlantic Ridge and northward to the Gakkel Ridge.

The African Plate had moved relatively slowly for the last 100 Ma or so in a general northeast direction with a speed estimated at around 2.15 cm (0.85 in) per year, drawing it closer to the Eurasian Plate. However, throughout this period, its continental interior has experienced many seismic changes such as long - term intra - continental crustal deformation which may be due to local and regional tectonic events occurring on the plate (Cloetingh and Burov, 2011; Zoback *et al*., 1993) and mantle - lithosphere interaction (Heine *et al*., 2008). Lack of effective seismic monitoring of the plate hampered the study of these events and seismic changes associated with it. To assess these seismic changes for the prediction of future occurrence of earthquakes in the African and parts of Eurasian plates, the knowledge of significant changes in *b*-value is essential. The *b*-value indicates the tectonic character of a region and has been assumed to depend on the accumulated stress in that region. Hence, this study intends to investigate the *b*-value variations in the African and parts of Eurasian Plates.

### 1.1 Tectonic Settings and Historical Seismicity

The African Plate's speed is estimated at around 2.15 cm (0.85 in) per year. It has been moving over the past 100 million years or so in a general northeast direction, drawing it closer to the Eurasian Plate. The African Plate (Fig.1) is rifting in the eastern interior of the African continent along the East African Rift. This rift zone represents a zone of maximum weakness where the African Plate is deforming, as plates to its east are moving rapidly northward.

The highest seismicity of the African continent is concentrated in East Africa. Recent seismicity demonstrates that the East African rift is prone to large earthquakes, since some of the strongest events of the 20$^{th}$ century exceeded $M$ = 7, such as that of the 13 December, 1910; Rukwa, Tanzania ($MS$ = 7.4), 20 and 24 May 1990, Sudan ($MS$ = 7.0 - 7.4), and 22 February 2006, Mozambique ($MW$ = 7.0) (Mourabit *et al*., 2013).

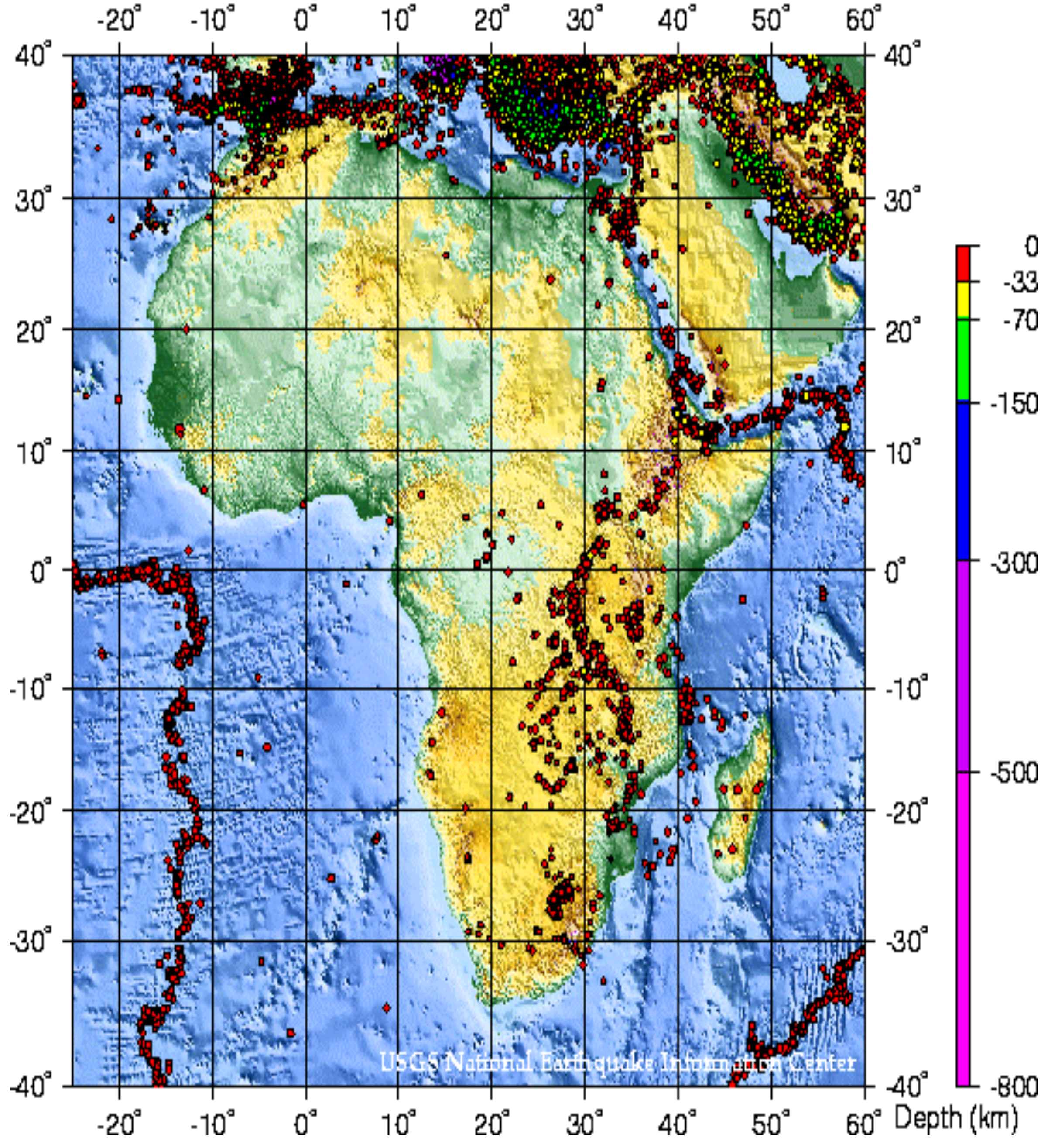


Figure 1: Seismicity Map of the Study Area [Source: National Earthquake Information Center (NEIC), US Geological Service.]

In North Africa, Algeria is known as one of the most active region because several large and shallow depth (0 – 30 km) earthquakes have occurred in the last six decades [Orléanville, (1954, *MS* = 6.0), El Asnam, (1980, *M* 7.3), Constantine (1985, *MS* 6.0), Tipasa - Chénoua (1989, *MS* 6.0), Mascara, (1994, *M* 6.0) and Zemmouri, (2003, *M* 6.8)].

Large earthquakes have also been reported in countries such as Morocco, Libya, and Egypt. In February 2004, the city of Al Hoceima and the Rif Mountains of Morocco were struck by a large earthquake (*MW*= 6.4), 10 years after the May 1994 (*MS* = 6.0) event. The city of Cairo in Egypt was struck in October 1992 by an earthquake of magnitude 5.8, which caused large damage. In 1935, the Syrte region in Libya experienced an earthquake of magnitude 6.9 with severe damage (Suleiman and Doser 1995; Suleiman *et al*., 2004).

Seismic activities in Southern Africa are believed to be an extension of the East Africa rift system. South Africa has experienced few major earthquake events. Among these is the earthquake of Orange Free State in 1912. Historically, the most severe earthquake of magnitude 6.3 on the Richter scale occurred on 29 September 1969 in Ceres, 100 km northeast of Cape Town (Alabi *et al*., 2013).

Central and Western Africa, is generally considered as aseismic or having low seismicity. The biggest magnitude recorded is *MW* = 6.5 in Ghana and *MW* = 6.0 in Cameroon. Though Nigeria is not located within the major earthquake zones of the world, nevertheless it has experienced series of earth tremors especially in the southwestern part. The first reported occurrence of an earth tremor in Nigeria was in 1939 in Lagos, Ibadan and Ile - Ife located in the south - western part of the country. Subsequent occurrences of earth tremors in Nigeria were in 1984, 1988, 1990, 1997, 2000 and 2006. The intensities of these shocks ranged from III to IV on the Modified Mercalli Intensity Scale (Akpan and Yakubu ,2010).

Several seismic events have also occurred in Accra, Ghana, extending along the Akwapin faults to the Volta River (Burke, 1969). In the past 120 years, Accra has on three occasions been damaged by major earthquakes in 1906, 1939, and 1941 (Junner, 1941).

On December 22, 1983, a large earthquake also occurred in Guinea further west of Nigeria in an area, which was previously considered aseismic (USGS location 11.93 S and 13.60 W) (Dorbarth *et al*., 1983). Seiberg (1932) also reported five earthquakes from Cameroon of which two were associated with the Cameroon mountain volcano and two including the largest had epicenters at Kribi (100 E, 40 N), 200 km to the south.

### 1.2 The *b*-value

In the year 1956, Charles Francis Richter and Beno Gutenberg proposed the relationship between earthquake magnitude and frequency in what they called the Gutenberg-Richter relation. This Gutenberg-Richter relation which is also known as the Frequency-Magnitude Distribution (FMD) is commonly used in the modeling of earthquake hazard, mostly related to the earthquake precursors and probabilistic seismic hazard assessments (Nuannin, 2006; Damanik *et al*., 2010). The FMD describes the number of earthquakes occurring in a given region as a function of their magnitude *M* as:

$$\log N = a - bM \tag{1}$$

where *N* is the cumulative number of earthquakes with magnitudes equal to or greater than *M*, and *a* and *b* are real constants whose values varies in time and space. The parameter $a$ characterizes the general level of seismicity in a given area during the study period, that is the higher the *a* value, the higher the seismicity. The parameter *b* commonly called the *b*-value has been widely used in the studies of seismicity, tectonics, seismic risk estimation and earthquakes prediction. The *b*-value indicates the tectonic character of a region and assumed to depend on the accumulated stress in that region (Nuannin, 2006). Schorlemmer *et al.* (2004) described *b*-value as a stress meter, depending inversely on the differential stress.

Regionally, changes in *b*-value are believed to be inversely related to changes in the stress level (Bufe, 1970; Gibowicz, 1973). An increase of applied shear stress or effective stress results in decrease of *b*-value (Urbancic *et al*., 1992; Wyss, 1973). A smaller *b*-value probably means that the stress is high in the examined region. Decreasing *b*-value within the seismogenic volume under consideration has been found to correlate with increasing effective stress levels prior to major shocks (Kanamori, 1981). Studies revealed that the *b*-value is also related to the depth of occurrence of the earthquake (Weimer and Benoit, 1996; Mori and Abercrombie, 1997; Wyss *et al*., 1997, 2001).

In general, the *b*-value in broad seismic regions is close to 1.0 from global statistics (Lay and Wallace, 1995). For regions in smaller scale over a few to tens of kilometers, the temporal and spatial variations in *b*-values may be significantly large, ranging from 0.5 to 1.5 in Japan (Ogata and Katsura, 1993) and from 0.5 to 1.3 near Parkfield of the San Andreas fault (Schorlemmer *et al*., 2004). Variation of *b*-value in a region is commonly correlated with characteristics of regional seismic activities. For example, high seismicity in magma chambers may be characterized by high *b*-values (Sanchez *et al*., 2004; Wiemer and McNutt, 1997). The initial rupture of large earthquakes, by contrast, was found to occur in regions where *b*-values were low (Wyss and Stefansson, 2006; Wyss *et al*., 2000). Schorlemmer *et al*. (2005) pointed out that the region with low *b*-value implies large differential stress and suggests its being toward the end of the seismic cycle. Such relationship can be applied for evaluating seismic hazard and earthquake forecasting (Smith, 1981).
The *b*-value in Equation (1) can be estimated either by linear least squares regression or by maximum - likelihood method (Aki, 1965; Ustu, 1965; Bender, 1983; Nuannin, 2006; Damanik *et al*., 2010). In this study, the maximum - likelihood method has been used to calculate *b*-value. The maximum - likelihood estimate of the *b*-value is given as (Öztürk, 2012):

$$b = 2.303M - M\,min + 0.005 \tag{2}$$

where $M$ indicates the average magnitude and $Mmin$ is the minimum magnitude of the local catalog data that is being investigated. Value 0.005 in Equation 2 is a correction constant.

## 2.0 DATA ACQUISITION, DESCRIPTION AND METHOD.

Earthquake data used for this study were extracted from the Advanced National Seismic System (ANSS) Comprehensive Catalog, a website of Northern California Earthquake Data Centre (NCEDC), USA (http://quake.geo.berkeley.edu/anss/catalog-search.html). The data covered a region bounded by latitudes -40° to +40° and longitudes -20° to +60° which comprises of the African and parts of Eurasian plates. The data were obtained in a readable format for earthquakes with magnitude and depth ranging from $MW = 2.0$ to $MW = 7.7$ and 0 to 700 km respectively, for a period of forty years (1/8/1975 to 31/7/2015). There were 73,389 earthquakes in all. Each datum composed the date of occurrence of earthquake, origin time, coordinates of epicenter, magnitude, event identification, and focal depth of earthquake.

### 2.1 Frequency – Magnitude Distribution (FMD) of Earthquakes

The Frequency – Magnitude Distribution (FMD) of earthquakes that took place in the study area for the forty-year periods of study was evaluated. This was done by plotting the cumulative number of earthquakes as a function of their magnitudes. These plots were then fitted with a straight line that best fit the plots. The straight line represents the Gutenberg – Richter equation. The magnitude of completeness $MC$ of the earthquake catalogue also known as the threshold magnitude which is the magnitude above which all earthquakes were recorded was then determined from the plots. The overall $b$-value of earthquakes from the study area was determined by finding the slope of the line of best fit while the $a$-value, that is, the seismicity level of the study area was also determined by substituting the known parameters into the Gutenberg – Richter equation. Figure 2 showed the Frequency – Magnitude Distribution of earthquakes in the study area for the forty-year periods of study. From Figure 2, we have $MC = 4.7$, $b = 1.18$, and $a = 10.4$.

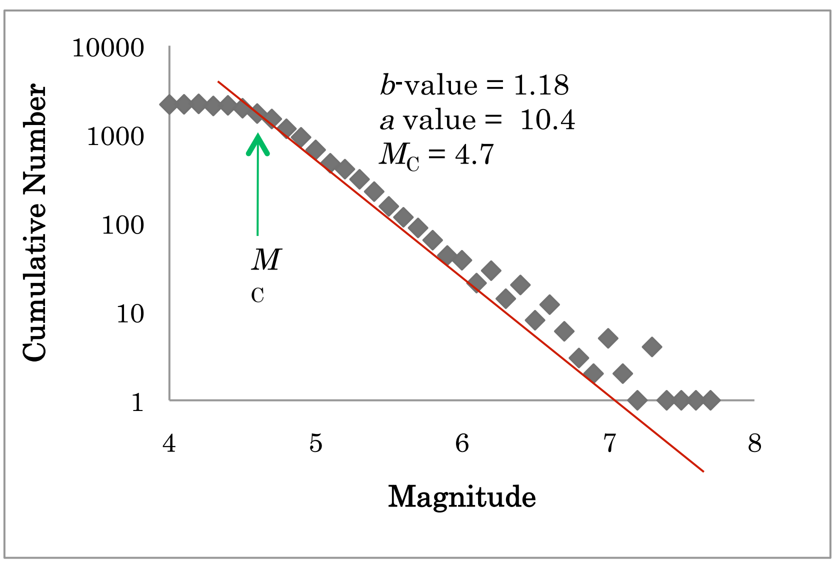


Figure 2: Frequency – Magnitude Distribution (FMD) of Earthquakes from August 1, 1975 to July 31, 2015. The Red Thin

## 2.2 Temporal Variation of *b*-value

To study variations of *b*-value with time, a sliding time window method was used. Due to high difference between the numbers of events in each window, constant number of events in each window was considered. A group of earthquakes was chosen from the earthquake catalogue and the *b*-value was calculated for the first window using the maximum likelihood equation. The window was then shifted by a time corresponding to certain number of events. The *b*-value was calculated for the new group of data and the process was repeated until the last window was reached. For this study, 100 events in windows have been selected which was shifted for every year. Several tests were performed by varying the number of events in the window i.e. 50, 100, 150 and 200. Varying the step (shift) length was also tested but it does not affect the resolution.

Figures 3, 4, 5 and 6 showed the temporal variations of *b*-values for ten years each of the periods of study while Figure 7 showed the temporal variation of *b*-values for the forty – year periods of study.

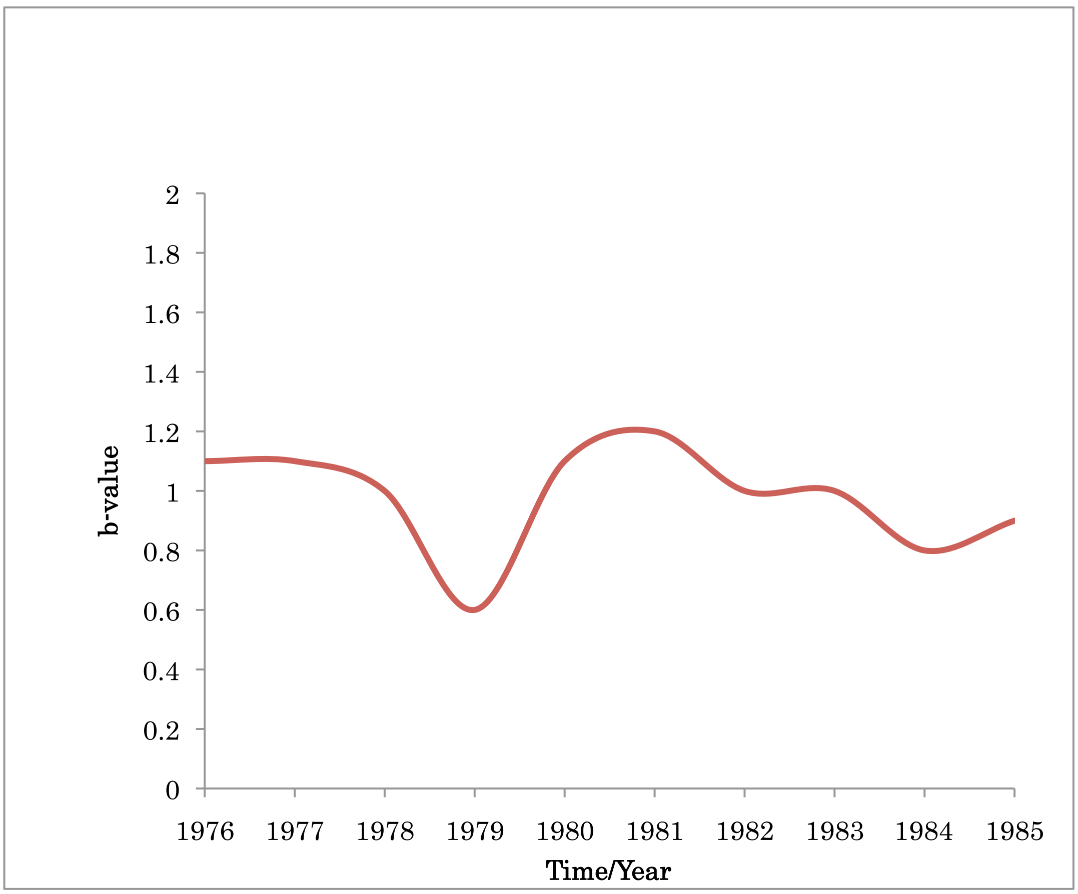


Figure 3: Temporal Variation of *b*-value from August 1, 1975 to July 31, 1985.

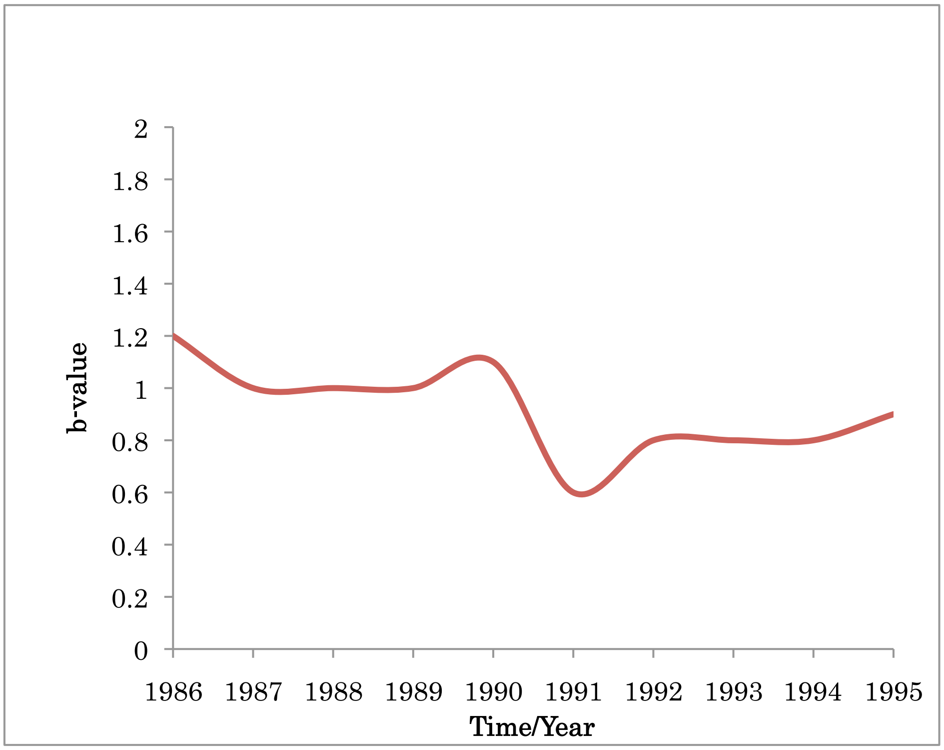


Figure 4: Temporal Variation of *b*-value from August 1, 1985 to July 31, 1995.

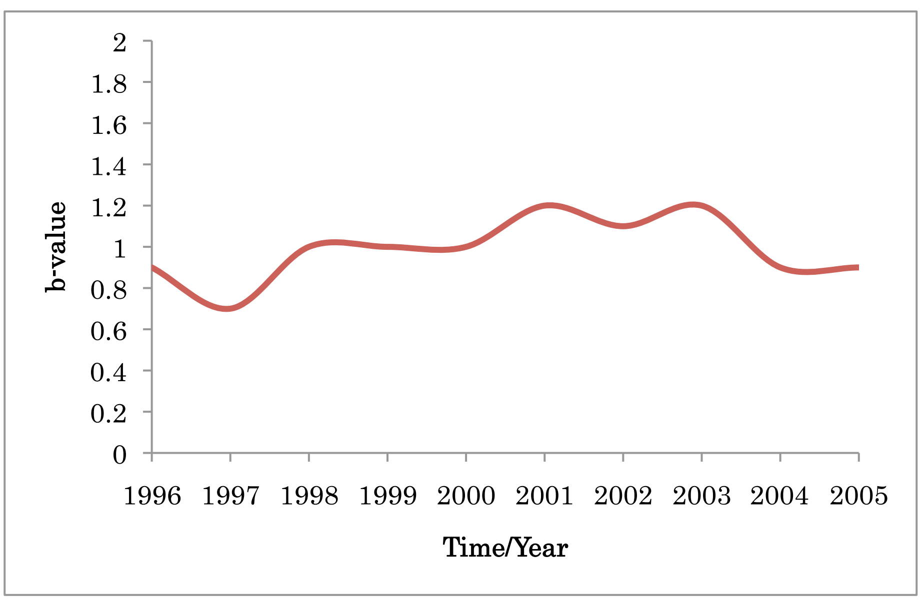


Figure 5: Temporal Variation of *b*-value from August 1, 1995 to July 31, 2005.

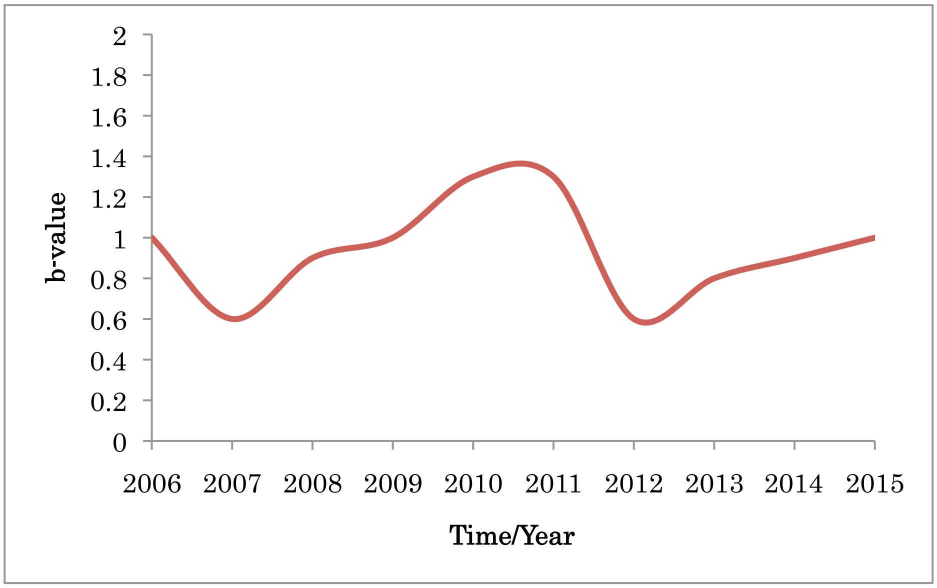


Figure 6: Temporal Variation of *b*-value from August 1, 2005 to July 31, 2015.

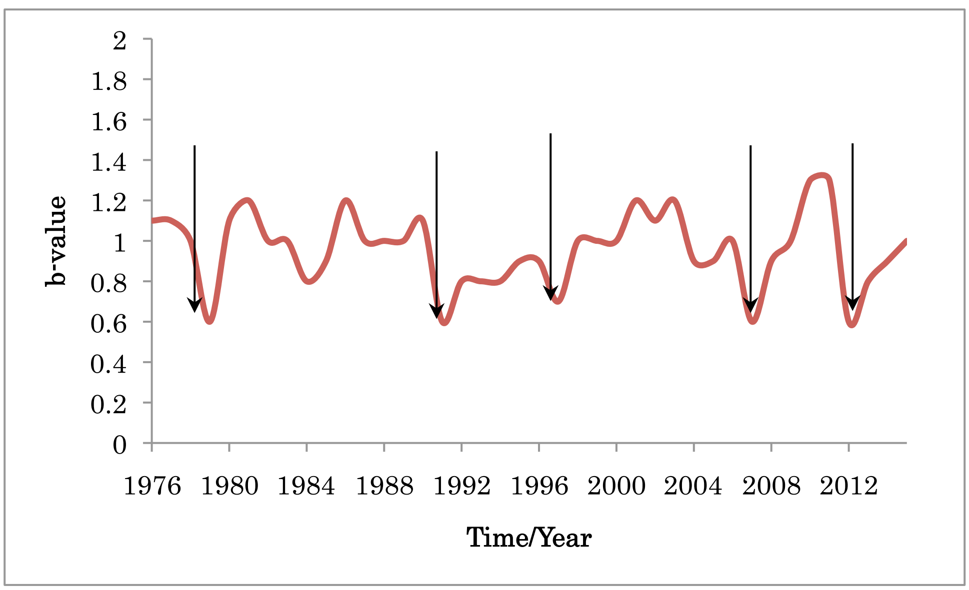


Figure 7: Temporal Variation of *b*-value from August 1, 1975 to July 31, 2015 as Thick Red Line. Arrows Mark the Occurrence Time of Large Earthquakes (*M ≥5.4*)

### 2.3 Spatial Variation of *b*-value

The spatial variation of *b*-values was mapped by projecting earthquake epicenters onto a plane. The study area was divided into grids and *b*-values were calculated for each grid using constant radius and constant number of events. In this study, the spatial variation of *b*-value was determined using a $10^{o}$ x $10^{o}$ processing grid with each grid containing a total of 100 events. To visualize the variation of *b*-value with space, the *b*-values were gridded using minimum curvature gridding method and were displayed using a color-shaded map. Figure 8 showed the spatial variation of *b*-values for the study area.

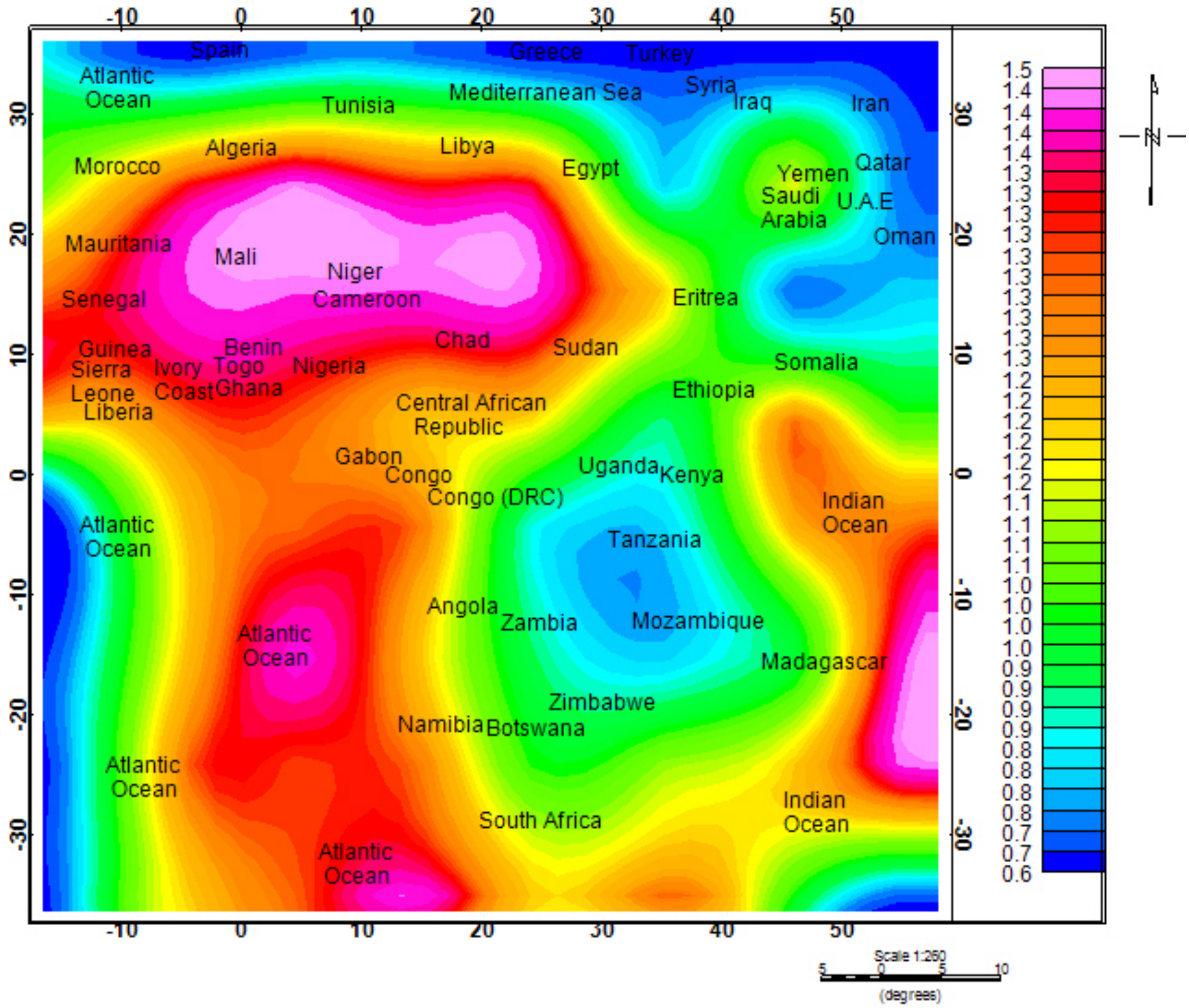


Figure 8: Spatial Variation of *b*-values for the Forty – Year Period of Study.

## 3.0 RESULTS AND DISCUSSION

The overall *b*-value of earthquakes from the study area for the entire periods of study was estimated to be 1.18 as shown in Figure 2. From the temporal variations of *b*-values (Figures 3, 4, 5, 6, and 7), it was observed that the *b*-value varies between 0.6 and 1.3 throughout the study period. High *b*-values were observed in the years 1976, 1977, 1980, 1981, 1986, 1990, 2001, 2002, 2003, 2010 and 2011. In these years the *b*-values ranges from 1.1 to 1.3. These years have the lowest average magnitude of earthquakes (between 4.1 and 4.4) as they were dominated by numerous earthquakes of small magnitudes.

The years 1978, 1982, 1983, 1984, 1985, 1987, 1988, 1989, 1992, 1993, 1994, 1995, 1996, 1998, 1999, 2000, 2004, 2005, 2006, 2008, 2009, 2013, 2014 and 2015 experienced a slight decrease in *b*-value. For these years, *b*-values vary between 0.8 and 1.0. The average magnitude of earthquakes that took place during these periods was between 4.5 and 4.9. These years were dominated by few earthquakes of large magnitudes.

The lowest *b*-values observed were between 0.6 and 0.7 and were recorded in the years 1979, 1991, 1997, 2007 and 2012. These years experienced the highest average magnitude of earthquakes (between 5.0 and 5.5) as they were dominated by numerous earthquakes of large magnitudes.

From the spatial variation of *b*-values (Fig. 8), we found the clustering of low *b*-value along the African – Eurasian plate boundary, in countries such as Spain, Greece and Turkey as well as parts of Atlantic and Indian Oceans. All these areas were shown in blue color and they have variations of *b*-values ranging from 0.6 to 0.7. Low *b*-values were also observed in some East African countries such as Uganda, Kenya, Tanzania, Zambia, Mozambique and Zimbabwe as well as some Arabian countries such as Syria, Iraq, Iran, Qatar, United Arab Emirates and Omar. These areas were shown in light blue color and they have variations of *b*-values ranging from 0.8 to 0.9. These areas have high level of seismicity and have experienced numerous earthquakes of large magnitudes. The average magnitude of earthquakes that took place in these region ranges from 4.6 to 5.5.

The areas marked by green color in the *b*-value distribution map are those areas that experienced just few earthquakes of intermediate magnitudes. The *b*-value for these regions ranges from 1.0 to 1.1. The average magnitude of earthquakes that took place in these regions was between 4.3 and 4.6. These areas include Tunisia, Egypt, Yemen, Saudi Arabia, Eritrea, Somalia, Ethiopia, Congo (DRC), Angola, Botswana, Madagascar and South Africa as well as parts of Indian and Atlantic Oceans.
Areas shown in yellow are areas of high *b*-values. These areas have low seismicity as they were dominated with numerous earthquakes of small magnitudes. The *b*-value for these areas ranges from 1.2 to 1.3 and the average magnitudes of earthquakes that took place in these regions was between 4.1 and 4.3. These areas include Morocco, Algeria, Libya, Namibia, Congo, Gabon, Central African Republic, Sudan, Chad, Nigeria, Ghana, Ivory Coast, Sierra Leone, Liberia, Guinea, Senegal and Mauritania.

The areas shown in pink represent areas of very low or no seismicity. These represent areas where the total number of earthquake that occurred was not up to the total number of earthquakes used for the calculation of *b*-value in this study or areas where no significant earthquake was recorded during the period of the study. The *b*-values for these regions range from 1.4 to 1.5. These areas include Benin, Togo, Cameroon, Mali and Niger and some parts of Indian and Atlantic Oceans.

## 4.0 CONCLUSION

The variation of *b*-value with time and space has been successfully investigated for earthquakes in the African and parts of Eurasian plates. Results obtained from the temporal variations of *b*-values showed that earthquakes of large magnitudes occurred when *b*-values were low throughout the study period while earthquakes of small magnitudes occurred when *b*-values were high. Significant drops in *b*-values revealed a U-shape curve in the *b*-value versus time graphs. A rapid increase of *b*-value with time was also observed after the occurrence of large earthquakes. Also, from the results obtained from the geographical distribution of *b*-values, it was observed that earthquakes of large magnitudes occurred in regions of low *b*-values while earthquakes of small magnitudes occurred in regions of high *b*-values. This study therefore concluded that the temporal and spatial variations of *b*-values might be considered as a precursor for earthquake prediction. Hence, this study suggests that monitoring the *b*-value variations in the African and parts of Eurasian plates may be a useful method for predicting likely occurrence of earthquakes in the study area.

## REFERENCES


Aki, K. 1965. Maximum - Likelihood Estimate of $b$ in the Formula $\log N = a - bM$ and Its Confidence Limits. *Bulletin of the Earthquake Research Institute* 43: 237 - 239

Alabi, A. A., Olukayode, D. A. and Adebambo A. 2013. Seismicity Pattern in Southern Africa from 1986 to 2009. *Earth Science Research* 2: 2

Akpan, O.U. and Yakubu, T.A. (2010) A Review of Earthquake Occurrences and Observations in Nigeria. *Earthquake Science*, **23**, 289-294.

Bufe, C. G. 1970. Frequency - Magnitude Variations during the 1970 Danville Earthquake Swarm. *Earthquake Notes* 41: 3 - 6

Burke, K. 1969. Seismic Areas of the Guinea Coast where Atlantic Fracture Zones Reach Africa. *Nature* 222 (5194): 655 - 657

Cloetingh, S. and Burov, E. 2011. Lithospheric Folding and Sedimentary Basin Evolution: A Review and Analysis of Formation Mechanisms. *Basin Research* 23: 257 – 290

Damanik, R., Andriansyah, Putra, H. K., Zen, M. T. 2010. Variations of *b*-values in the Indian Ocean – Australian Plate Subduction in South Java Sea. *Proceedings of the Bali 2010 International Geosciences Conference and Exposition, Bali, Indonesia*: 19 - 22

Dorbarth, L., R. Caulon, T. George, and P. Mougue. 1983. Guinean Earthquake of December 22, 1983. *Tectonophysics* 82: 112 – 124

Gibowicz, S. J. 1973. Variation of the Frequency-Magnitude Relation during Earthquake Sequences in New Zealand. *Bulletin of the Seismological Society of America* 63: 517 – 528

Pararas-Carayannis, G. 2011. The earthquake and tsunami of July 21, 365 AD in the Eastern Mediterranean Sea - Review of impact on the ancient world - assessment of recurrence and future impact. 30 (4): 286

Heine, C., Muller, R. D., Steinberger, B. 2008. Subsidence in Intra - continental Basins Due to Dynamic Topography. *Physics of the Earth and Planetary Interiors* 171: 252 – 264

Junner, N. R. 1941. The Accra Earthquake of 22nd June, 1939. *Gold Coast Geological Survey* 13

Kanamori, H. 1981. The Nature of Seismic Patterns before Large Earthquakes. In Earthquake Prediction: An International Review. *American Geophysical Union* 4: 1 - 19

Lay, T. and Wallace, T. C. 1995. Modern Global Seismology. Academic Press: 393

Mori, J., and R. E. Abercrombie 1997. Depth Dependence of Earthquake Frequency Magnitude Distributions in California: Implication for the Rupture Initiation. *Journal of Geophysical Research* 102: 15, 81 - 90

Mourabit, T., Abou Elenean, K., Ayadi, A., Benouar, D. and Ben Suleman, A. 2013. Neo - deterministic Seismic Hazard Assessment in North Africa. *Journal of Seismology*

Nuannin, P. 2006. The Potential of *b*-value Variations as Earthquake Precursors for Small and Large Events. *Digital Comprehensive Summaries of Uppsala Dissertations from the Faculty of Science and Technology*

Ogata, Y. and Katsura, K. 1993. Analysis of Temporal and Spatial Heterogeneity of Magnitude Frequency Distribution Inferred From Earthquake Catalogues. *Geophysical Journal International* 113: 727 – 738

Ozturk, S. 2012. Statistical Correlation Between *b*-value and Fractal Dimension Regarding Turkish Epicentre Distribution. *Earth Sciences Research Journal* 16: 103 - 108

Sanchez, J. J., McNutt, S. R., Power, J. A. and Wyss, M. 2004. Spatial Variations in the Frequency – Magnitude Distribution of Earthquakes at Mount Pinatubo volcano. *Bulletin of the Seismological Society of America* 94: 430 – 438

Schorlemmer, D., S. Wiemer, and M. Wyss 2004. Earthquake Statistics at Parkfield I: Stationarity of *b*-values. *Journal of Geophysical Research* 109

Schorlemmer, D., Wiemer, S., and Wyss, M. 2005. Variations in Earthquake Size Distribution across Different Stress Regimes. *Nature* 437 (22): 539 – 542

Seiberg, A. 1932. Handbuck der Geophysik. Berlin, Germany. *Seismological Society of America* 62: 435 – 687

Smith, W. D. 1981. The *b*-values as an Earthquake Precursor. *Nature* 289: 136 – 139

Suleiman A. S. and Doser D. I. 1995. The Seismicity, Seismotectonics and Earthquake Hazards of Libya, With Detailed Analysis of the 1935 April 19, $M$ = 7.1 Earthquake Sequence. *Geophysical Journal International* 120: 312 - 322

Suleiman A. S., Albini P. and Migliavacca P. 2004. A Short Introduction to Historical Earthquakes in Libya. *Annals of Geophysics* 47: 2 - 3, 545 - 554

Urbancic, T. I., C. I. Trifu, J. M. Long, and R.P. Young 1992. Space - Time Correlation of *b*-values with Stress Release: 449 - 462

Ustu, T. 1965. A Method in Determining the Value of $b$ in a formula $\log N = a - bM$ Showing the Magnitude Frequency For Earthquakes. *Geophysical Bulletin of Hokkaido University* 13: 99 – 103

Wiemer, S. and J. Benoit 1996. Mapping the *b*-value Anomaly at 100 km depth in the Alaska and New Zealand Subduction Zones. *Geophysical Research Letters* 23: 1557 - 1560

Wiemer, S. and McNutt, S. 1997. Variations in Frequency – Magnitude Distribution with Depth In Two Volcanic Areas: Mount St. Helens, Washington, and Mt. Spurr, Alaska. *Geophysical Research Lett*ers 24: 189 – 192

Wyss, M. 1973. Towards a Physical Understanding of Earthquake Frequency Distribution. *Geophysical Journal International* 31: 341 – 359

Wyss, M. and Stefansson, R. 2006. Nucleation Points of Recent Mainshocks in Southern Iceland, Mapped by *b*-values. *Bulletin of the Seismological Society of America* 96: 599 – 608

Wyss, M., F. Klein, K. Nagamine, and S. Wiemer 2001. Anomalously High *b*-values in the South Flank of Kilauea Volcano, Hawaii: Evidence for the Distribution of Magma below Kilauea's East Rift Zone. Journal of Volcanic and Geothermal Research 106: 23 - 37

Wyss, M., K. Shimazaki, and S. Wiemer 1997. Mapping Active Magma Chambers by *b*-value Beneath the Off - Ito Volcano, Japan. *Journal of Geophysical Research* 102: 20413 - 20422

Wyss, M., Schorlemmer, D. and Wiemer, S. 2000. Mapping Asperities by Minima of Local Recurrence Time: The San Jacinto - Elsinore Fault Zones. *Journal of Geophysical Research* 105: 7829 – 7844

Zoback, M. D., Stephenson, R. A., Cloetingh, S., Larsen, B. T., Vanhoorn, B., Robinson, A., Horvath, F., Puigdefabregas, C., Benavraham, Z., 1993. Stresses in the Lithosphere and Sedimentary Basin Formation. *Tectonophysics* 226: 1 – 13